1990

Theoretical Basis for Controlling Minimal Tumor Temperature During Interstitial Conductive Heat Therapy

Charles F. Babbs
Purdue University, babbs@purdue.edu

Neal E. Fearnot

J A. Marchosky

C J. Moran

James T. Jones

See next page for additional authors

Theoretical Basis for Controlling Minimal Tumor Temperature During Interstitial Conductive Heat Therapy

CHARLES F. BABBS, NEAL E. FEARNOT, MEMBER IEEE, J. A. MARCHOSKY, C. J. MORAN, JAMES T. JONES, AND T. D. PLANTENGA

C. F. Babbs, N. E. Fearnot, J. T. Jones, and T. D. Plantenga are with the Biomedical Engineering Center, Purdue University, West Lafayette, IN 41907.

J. A. Marchosky is with Neurological Associates, Chesterfield, MO 63017.

C. J. Moran is with Radiological Associates, Chesterfield, MO 63017.

ABSTRACT

This paper describes simulation of steady-state intratumoral temperatures achieved by a simple modality of local heat therapy: interstitial treatment with parallel arrays of warmed, conductive heating elements. During "conductive heating" power is directly deposited only in the interstitial probes. Adjacent tissue is warmed by heat conduction. Simulations of interstitial conductive heating involved solution of the bioheat transfer equation on a digital computer using a finite difference model of the treated tissue. The simulations suggest that when the complete temperature distributions for conductive interstitial hyperthermia are examined in detail, substantial uniformity of the temperature distributions is evident. Except for a thin sleeve of tissue surrounding each heating element, a broad, flat central valley of temperature elevation is achieved, with a well defined minimum temperature, very close to modal and median tissue temperatures. Because probes are inserted directly in tumor tissue, the thin sleeve of overheated tissue would not be expected to cause normal tissue complications. The temperature of the heated probes must be continuously controlled and increased in the face of increased blood flow in order to maintain minimum tumor temperature. However, correction for changes in blood flow is possible by adjusting probe temperature according to a feedback control scheme, in which power dissipation from each probe is the sensed input variable. Conductive interstitial heating with continually controlled probe temperature deserves investigation as a technique for local hyperthermia therapy.

1. INTRODUCTION

During the past decade, clinical use of hyperthermia therapy for cancer has accelerated. Reports from many institutions indicate that a significant number of patients for whom conventional radiation or chemotherapy has failed show dramatic tumor regressions in response to heat, either alone [1-4] or, most successfully, in combination with radiation [5-7]. Complete remission of local lesions can be obtained in 50-70% of patients with various superficially located, and thus easily heated, lesions when hyperthermia is combined with radiation therapy [8]. There are several possible mechanisms for the antitumor effects of heat. Cell culture studies suggest that malignant cells may be slightly more heat sensitive than normal cells [9-11]. In addition, solid tumor masses in vivo appear even more heat sensitive than cells from the same tumor line grown in vitro [12-13]. This selective effect may be the result of induced hypoxia and acidosis within the tumor mass, which together potentiate the effects of heat upon individual cells [12-14].

A major limitation to the success of hyperthermia therapy for malignancy is the failure to elevate intratumoral temperatures uniformly above a critical "kill level," often taken as 42°C. Dewhirst, Sim, and coworkers have shown a strong correlation of high variability in intratumoral temperature, in particular low minimum tumor temperature, with poor outcome of clinical hyperthermia treatment of spontaneous cancers in pet animals[16]. Cold spots may never reach therapeutic temperatures, and so remain viable after treatment. Unless energy is perfectly focused on neoplastic tissue only, hot spots in surrounding normal tissues lead to complications such as intolerable pain or ulceration of overlying skin. To avoid complications of hot spots, especially with external source techniques, the therapist is obliged to reduce total applied power, and as a result, mean tumor temperature is often below target [Fig. l (a)]. In our view, the technical goal of improved local heat therapy is to obtain more uniform, on-target intratumoral temperatures, as illustrated in Fig. 1 (b).

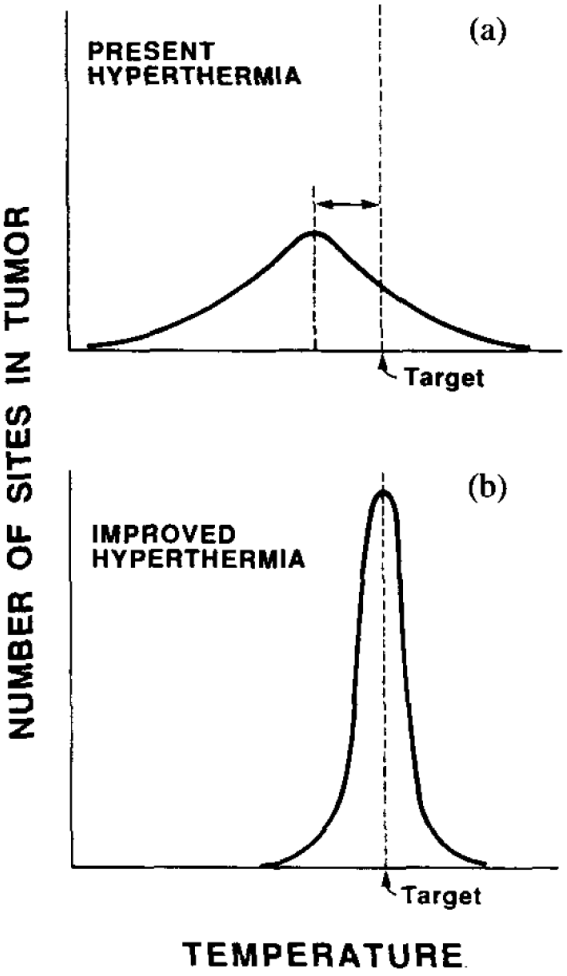

Fig. 1. Concept of present versus improved hyperthermia illustrated with histograms. Wide variation in intratumoral temperatures leads to hot spots and cold spots (top). In an attempt to minimize complications associated with hot spots, total power is limited such that mean temperature is less than the target temperature. In improved hyperthermia the standard deviation of intratumoral temperatures is reduced and mean temperature is on target.

Noninvasive external means of tissue heating, including microwave, inductively coupled radiofrequency, capacitively coupled radiofrequency, and high-intensity ultrasound all exhibit fundamental physical property of attenuation of absorbed power as a function of depth in tissue [17]. Skin, which is closest to the heat source, is typically overexposed, requiring surface cooling with water jackets or blouses that cover the treatment site. These impede patient monitoring. A variety of focusing schemes have been tried to improve heating of deeper lesions, including the

annular phased array of microwave applicators [18-20] and focused, high-intensity ultrasound, delivered by moving applicators or multiple beams [21-23]. None of these has yet to prove totally satisfactory [24].

Accordingly, increasing attention has been paid to interstitial techniques, in which power sources such as microwave antennas, or ferromagnetic seeds that are inductively heated by a high-frequency magnetic field are implanted directly in the substance of the tumor tissue [25]. Although interstitial methods are invasive, selective heat delivery to the tumor is superior. Power is delivered from within the tumor, sparing the surrounding normal tissues. Interstitial applicators include microwave antennae, electrodes for delivery of radiofrequency current, metallic composite materials that are excited by radiofrequency electric fields to produce heat, and ferromagnetic seeds, as well as the conductive heating elements described in this paper [25-29].

We now describe computer simulation of the simplest, and most easily controlled form of interstitial heating, in which the tumor is implanted with multiple needle-like probes that contain heating elements. The probes contain resistive heating elements that are hard wired to a bedside control unit. The core temperature of each probe is continually monitored and can be adjusted continuously under computer control. The probes are brought to a specified temperature, under computer control, and the substance of the tissue is warmed by conductive heat transfer. The kinds of temperature distributions produced are similar to those created by inductively heated ferromagnetic seeds [30-31].

The goals of the present modeling effort were to describe and characterize the temperature distributions created by the continuously controlled, conductive heating probes and to predict trade-offs required to achieve therapeutic temperatures in tumor tissue for various spacings of conductive heating elements in the presence of various values of tumor blood flow. Using a nonrectangular, offset probe spacing the simulations revealed a remarkable uniformity of steady-state temperatures in the regions between the probes. This paper describes the thermal properties of this potentially useful, and cost effective approach, and continues to suggest an easily implemented algorithm for automated adjustment of such a system in real time, to maximize the volume of tissue maintained at the target temperature, despite moment to moment changes in tumor blood flow.

1. COMPUTATIONAL METHODS

A. Approach

We modeled heat transfer during interstitial conductive heat therapy produced by a parallel array of implanted catheters, in which the spacing from any catheter to each of its six nearest neighbors is equal, forming a cross-sectional pattern of equilateral triangles. In this paper we refer to "catheter spacing" as the horizontal distance in centimeters between catheters in each staggered row (see Fig. 3), which is also equal to the line-of-site distance to the nearest catheter neighbors in the rows vertically above and below, owing to the triangular symmetry of the array.

In these simulations the catheters are maintained at a fixed, elevated temperature, as could be accomplished, for example, by feedback controlled resistive heating elements within the

catheters. Heat is transferred to the surrounding tissues by thermal diffusion. No energy is directly absorbed by tissue water, as in interstitial microwave heating. Tissue temperature is therefore maximum at the catheter surface and minimum near the center point between each triplet of catheters (except for the special case of zero blood flow when tissue temperature will equal interior catheter temperature). Digital modeling of temperature distributions for such a hyperthermia system is especially advantageous because the complete temperature distribution produced by such an array would be difficult to obtain experimentally. Thermometry with implanted sensors in animal or clinical studies can sample temperature at only a few discrete points. Such samplings can be especially misleading when high thermal gradients are involved, as in the present case of conductive heating.

Steady-state temperature distributions produced by interstitial conductive heating of tissue were characterized using finite difference solutions of the bioheat transfer equation, performed numerically on a Dual VAX 11/780 mainframe computer, implementing the iterative method of successive over-relaxation (SOR) [32-33]. The iterative method began with a guessed initial temperature distribution, and sequentially improved the temperatures on successive iterations until the steady-state bioheat equation was satisfied. Potentially faster approaches, including the alternating-direction-implicit (ADI) procedure and the Fourier analysis-cyclic-reduction procedure were explored and found either ill suited to the present problem, or no faster than the SOR method for the boundary conditions of interstitial conductive heating.

To reduce the modeling problem to two dimensions, a virtual plane perpendicular to the axes of the catheters at their midpoints was studied. The length of the heated segment was assumed to be much greater than the spacing between catheters. Steady-state temperature was calculated for each node of a finely spaced grid in the plane. The steady-state temperature, rather than the transient response, was studied, since parallel clinical trials with a similar system utilized treatment durations of several hours. Thus, steady-state temperatures are the clinically relevant ones in conductive heat therapy.

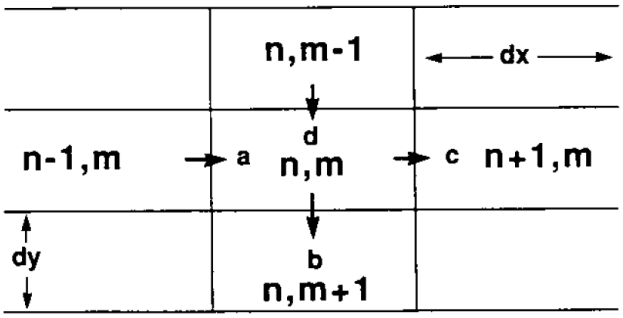

Fig. 2. Definition of control volumes for heat transfer model. The volume of each node is L dx dy. Conductive heat transfer terms a, b, c. and d, required for energy balance are indicated by arrows. Length, L, is perpendicular to the plane of the page.

B. Calculations

Derivation of computational formulae is illustrated for the case of an interior node (not adjacent to an adiabatic boundary) in a rectangular slab of tissue. Each node represents a control volume of length L and cross sectional dimensions Δx and Δy , with $L >> \Delta x$ or Δy. The volume of each node is $L\ \Delta x\ \Delta y$. Conductive heat transfer into and out of mode n, m is represented by the four quantities a, b, c, and d (Fig. 2).

The expression for the energy balance in each control volume, heat into control volume = heat out of control volume at steady state is of the form

$$a + d = wc_b(T_{n,m} - T_a)L\ \Delta x\ \Delta y + b + c \quad ,$$

where w is the specific perfusion per unit volume of tissue, c_b is the specific heat of blood and $T_{n,m} - T_a$ represents the steady-state temperature rise of the control volume above arterial blood temperature T_a. The heat loss term due to blood perfusion is the classical expression in the bioheat equation, which has been studied and validated by Chen and Holmes [34]. In the conductive heating problem there is no power absorption term, and metabolic heat generation of the tissue is assumed to be negligible. The conductive heat transfer terms are

$$\begin{aligned} a &= k\ \Delta y L(T_{n-1,m} - T_{n,m})/\Delta x \\ b &= k\ \Delta x L(T_{n,m} - T_{n,m+1})/\Delta y \\ c &= k\ \Delta y L(T_{n,m} - T_{n+1,m})/\Delta x \\ d &= k\ \Delta x L(T_{n,m-1} - T_{n,m})/\Delta y \end{aligned} \quad ,$$

where k is the thermal conductivity of tissue. We seek to solve this energy balance equation for the temperature at node n, m as a function of the surrounding temperatures and the local blood flow. Substituting, and dividing by $L\ \Delta x\ \Delta y$, we have

$$\begin{aligned} k(T_{n-1,m} - T_{n,m})/(\Delta x)^2 + k(T_{n,m-1} - T_{n,m})/(\Delta y)^2 \\ = wc_b(T_{n,m} - T_a) + k(T_{n,m} - T_{n,m+1})/(\Delta y)^2 \\ + k(T_{n,m} - T_{n+1,m})/(\Delta x)^2 \end{aligned} \quad .$$

Making the change of variable, temperature rise = $\theta = T - T_a$,

$$wc_b\theta_{n,m} + \frac{k}{(\Delta x)^2}(\theta_{n,m} - \theta_{n+1,m} - \theta_{n-1,m} + \theta_{n,m})$$

$$+ \frac{k}{(\Delta y)^2}(\theta_{n,m} - \theta_{n,m+1} - \theta_{n,m-1} + \theta_{n,m}) = 0.$$

Solving for θ in terms of the surrounding temperatures and blood flow,

$$\theta_{n,m} = \frac{\frac{k}{(\Delta x)^2}(\theta_{n+1,m} + \theta_{n-1,m}) + \frac{k}{(\Delta y)^2}(\theta_{n,m+1} + \theta_{n,m-1})}{wc_b + 2k/(\Delta x)^2 + 2k/(\Delta y)^2}.$$

In the particular case in which $\Delta x = \Delta y$, this expression reduces to

$$\theta_{n,m} = \frac{\theta_{n+1,m} + \theta_{n-1,m} + \theta_{n,m+1} + \theta_{n,m-1}}{wc_b \frac{(\Delta x)^2}{k} + 4}.$$

Note that for the case of perfusion, $w = 0$, θ is the average of temperatures in surrounding nodes, the standard formula for iterative solution of the heat equation without perfusion [32].

A similar analysis was performed for nodes along adiabatic boundaries and for corner nodes having two adiabatic boundaries. Boundary nodes have one half the volume of interior nodes, and the adiabatic corner node has one quarter of the volume. The conductive heat transfer across the adiabatic boundaries is zero.

Given expressions of this form for the temperature rise at each node, the computational strategy for numerical approximation of the steady-state temperature distribution begins by defining nodes that represent heaters and nodes that represent surrounding perfused tissue. After heater nodes are set at the target temperature ($\theta = T_{target} - T_a$) and tissue nodes at the arterial temperature ($\theta = 0$), as an initial guessed solution, $\theta_{n,m}$ is calculated iteratively for all nodes in succession. The gradual diffusion of heat into the tissue is mimicked by the general rise in temperature toward steady-state levels. Computation of consistently stable values indicates convergence. The rate of convergence was enhanced by successive over-relaxation according to the expression

$$\theta_{n,m} = \theta_{n,m} + \alpha(\theta_{n,m} - \theta_{\text{last}}),$$

where θ_{last} is the previously calculated temperature rise. Judicious selection of $0 < \alpha < 1$ allows much faster convergence in most cases. (Here α equals s $\Omega - 1$, were Ω is the successive over-relaxation coefficient defined in [32].)

For the simulations subsequently reported we selected mesh sizes of 0.05 cm or less and α's for most rapid convergence, ranging from 0.85 to 0.96. The treatment field is a rectangular grid of n x n nodes where n was between 50 and 200, making 2500 to 40 000 nodes. For large volume simulations nodes were placed 0.5 mm apart and the entire modeled space of 100 x 100 nodes represented a 5 x 5 cm cross-sectional area. Variation in the spacing of heating elements and variation in tissue blood flow were simulated to delineate the effects of these variables upon tissue temperature distributions. This approach allowed generation of both relief maps and histograms of temperature distributions within the treated region. The histograms displayed the complete temperature distributions in a simple, two-dimensional format. To better study the temperature distributions while minimizing computation time, three related simulation programs were developed.

I) Large Volume, Low Resolution Simulation: This simulation program was used to calculate steady-state temperatures in a cross section of tissue several centimeters in horizontal and vertical dimensions, containing 23 parallel heating elements, assuming midplane horizontal and vertical symmetry. The planes of symmetry were located at $x = 0$ and $y = 0$, and represent adiabatic boundaries due to symmetry. A representative model space with origin at (0, 0) is shown in Fig. 3, for 1.0 cm spacing. The right, lower quadrant of a symmetrical array of 23 heating elements with horizontal rows 1.0 cm apart and vertical rows 0.85 cm apart is illustrated. Adiabatic boundaries, corresponding to planes of symmetry, are located at $x = 0$ and $y = 0$. The mesh size is $\Delta x = \Delta y = 0.05$ cm in this example of 1.0 cm probe spacing. The circular profiles of the heating elements are roughly approximated by the cross-like clusters of 12 nodes each. Temperatures in these heater nodes were clamped at 5 °C above arterial blood temperature to simulate the action of the feedback controlled conductive heating catheters. The complete model space extends to $x = 5$ cm, $y = 5$ cm. Exterior boundaries of the model space are clamped at arterial blood temperature.

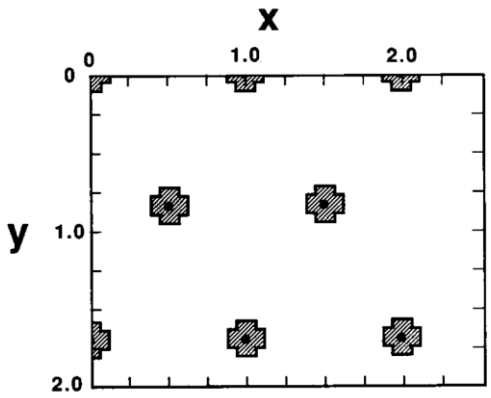

Fig. 3. Workspace of low resolution thermal model illustrated for 1.0 cm horizontal probe spacing. Horizontal (x) and vertical (y) units are in centimeters. The workspace includes one quadrant of the treated area. Interstitial conductive heating probes are represented by shaded zones, which are maintained at a fixed, target temperature. In this example the staggered rows of probes have 1.0 cm horizontal separation and 0.866 cm nominal (0.85 cm actual) vertical separation center to center. Each small box represents one node, 0.05 x 0.05 cm in dimensions. Similar model spaces were studied for 1.5 and 2.0 cm probe spacing. "Catheter spacing" is defined as the horizontal distance in centimeters between catheters in each staggered row, which is also equal to the line-of-site distance between catheters.

2) Small Volume, High Resolution Simulation: Early results of the first simulation program showed that most of the temperatures for interior parts of an array of conductive heating elements form a repeating, symmetrical pattern of peaks and high valleys. Because the ridge lines between peaks form adiabatic boundaries, the temperatures for all the high thermal valleys except the outermost ones are the same, provided heater spacing and blood flow are uniform.

After identifying the adiabatic boundaries caused by the symmetry of the catheter arrangement, it was possible to simulate temperatures in the region surrounding an interior catheter to obtain higher resolution of 0.1 mm between nodes with the same 100 x 100 grid size. A segment surrounded by adiabatic boundaries includes quadrants of two heaters at diagonally opposite comers (Fig. 4). An interior "valley" of the temperature distributions between diagonally adjacent thermal peaks is defined by planes of symmetry that run along the "ridge" lines formed by the rows and columns of heating elements, as shown in Fig. 3. These planes correspond to adiabatic boundaries since $dT/dx = 0$ everywhere for vertical ridge lines, and since $dT/dy = 0$ everywhere for horizontal ridge lines. A sketch of the high resolution model space for an interior valley is presented in Fig. 4. The heaters in cross section are quarter circles of user-specified radius r. The results are representative of all other segments on the interior of the array. Results of this simulation program allowed us to investigate most efficiently the relationships among steady-state power, blood flow, and minimum "valley" temperature, which might be usefully exploited in an advanced, feedback controlled conductive heating system.

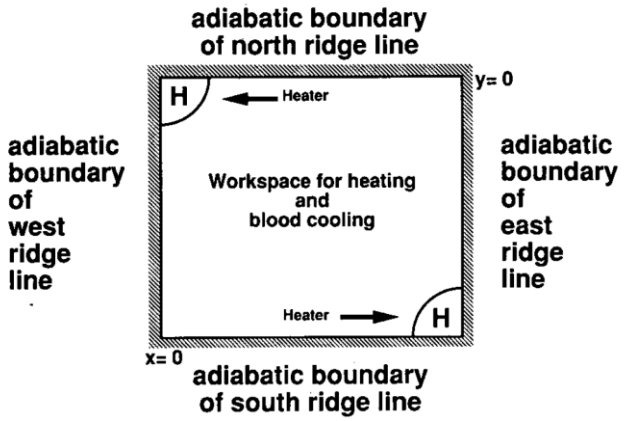

Fig. 4. Workspace of high resolution thermal model of interior region of interstitial probe array (approximately to scale). Quadrants of interstitial conductive heating probes are shown in cross section at diagonally opposite corners.

3) Software for Comparison of Minimum Temperatures: This program allowed evaluation of the effects of heater spacing, blood flow, and target temperature upon the effectiveness of tissue heating in an interior valley, as described by the thermal "droop": $(T_{target} - T_{min})/(T_{target} - T_a)$ where T_{min} is the minimum (valley floor) temperature, Target is the heater set point, and T_a, is arterial blood temperature. The importance of minimum intratumoral temperatures as a predictor of the success of hyperthermia therapy has been recently highlighted by the work of Dewhirst, Sim, and co-workers [16]. Additionally, steady-state power is calculated from the steady-state heat loss from the simulated catheter, so that it is possible to relate power to blood flow and T_{min} for any chosen catheter spacing. Knowledge of these relationships allows compensation for changing blood flow during hyperthermia treatment, based upon the power emitted from each probe.

3. RESULTS

A. General Features of Temperature Distributions

Fig. 5 illustrates the general features of temperature distributions produced by conductive heating in these simulations. These temperature distributions may be considered to represent those in a real system obtained near the midpoint of the active, heated length of the array of elements, and to correspond to a cross section through the center of the tumor, perpendicular to the individual heating elements. Fig. 5(a) is a hidden line, three-dimensional plot of the temperature distribution within the model space shown in Fig. 3 with 1.0 cm catheter spacing. The basal plane of the plot represents the right lower quadrant of a cross section through the treated tissue. The temperature at each point in the plane is represented as the height of the curved surface above the basal plane. Fig. 5(b) illustrates east-west slices taken through the surface shown in Fig. 5(a). The continuous temperature curves represent temperatures at successive y levels from y = 0 to y = 0.425 cm, midway between two rows of heating elements.

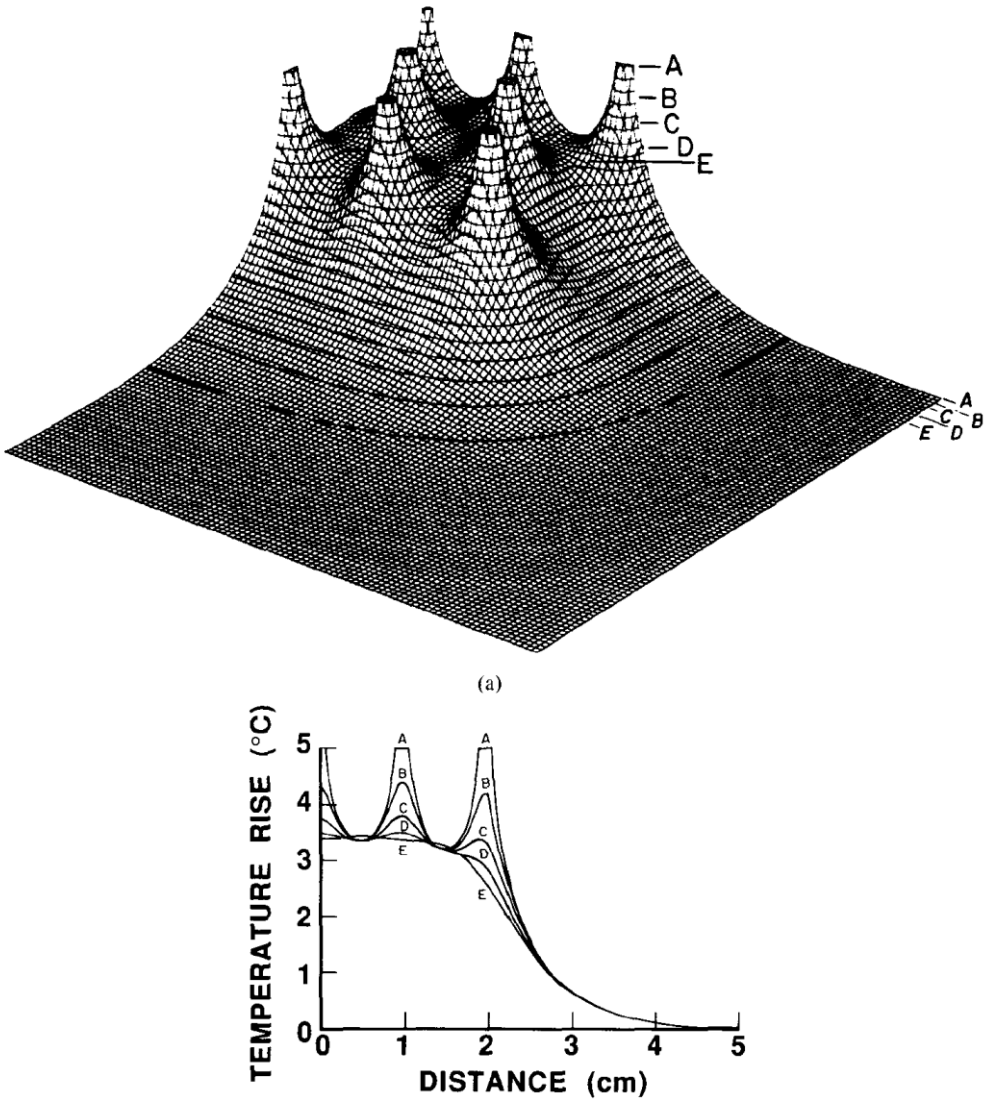

Fig. 5. Low resolution simulation for "typical" parameters, flow = 0.2 mL/min/g, horizontal spacing = 1.0 cm. Probe temperature = 5.0 °C greater than arterial blood temperature. External edge temperature = arterial blood temperature. Probe diameter 0.2 cm. Mesh size = 0.05 cm. (α = 0.85. Tolerance = 0.001 C. (a) Three-dimensional hidden-line plot showing south east quadrant of 23 probe array. East face is bottom right. South face is bottom left. The curved surface represents the temperature rise above arterial blood temperature. (b) Standard plot with five horizontal (east-west) slices through array of Fig. 5(a) at levels y = 0, 0.10625, 0.2125, 0.31875, and 0.425. Outside the array of heated probes temperature drops gradually to the level of arterial blood temperature, represented as zero on the vertical axis.

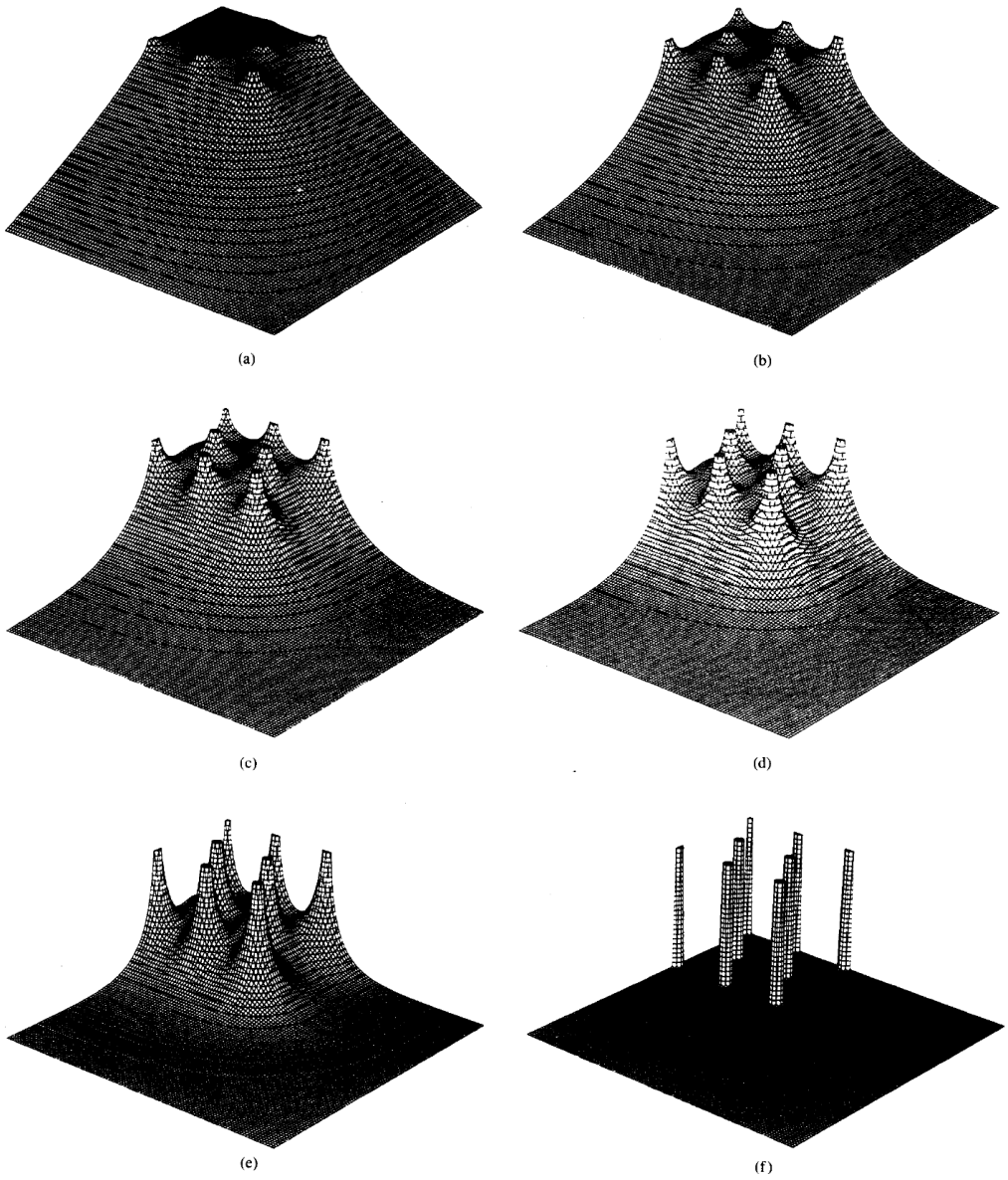

Fig. 6. (a) Low resolution output for zero blood flow. Other details similar to Fig. 5(a). Temperature at outer edges of basal plane is forced to equal arterial blood temperature. All heat loss occurs via conduction toward these cooled edges. (b) Output for blood flow = 0.05 mL/min/g. Other details similar to (a). (c) Output for blood flow = 0.10 mL/min/g. Other details similar to (a). (d) Output for blood flow = 0.20 mL/min/g. Other details similar to (a). (e) Output for blood flow = 0.50 mL/min/g. Other details similar to (a). (f) Output for "infinite" blood flow (9999 mL/min/g). Other details similar to (a).

Fig. 6(a)-(f) illustrate the influence of blood flow in the tissue upon the altitude of the high valley floors (minimum temperature elevation in the tissue). For a given probe spacing, the major determinant of minimal tumor temperature is local blood flow. The greater the blood flow, the lower the temperature in the high valleys. If flow equals zero, interior valley temperature within the array of heaters approaches the heater set point [Fig. 6(a)]. As blood flow approaches infinity, interior valley temperature approaches that of arterial blood [Fig. 6(f)]. Fig. 6(b)-(e) illustrate the topography of the thermal valleys for blood flows ranging from 0.05 to 0.5 mL/min/g, the range anticipated for most tumors.

B. High Resolution and Histogram Analysis of the Effects of Heater Spacing and Blood Flow

Fig. 7(a) shows a panoramic view of the temperatures in the region surrounding a single interior heating element. Fig. 7(b) is the corresponding histogram output. The ‘‘probability density” function plotted on the vertical axis is the frequency of nodes in a given temperature interval ΔT, scaled such that the area under the complete histogram is unity. The proportion of tissue for which temperature lies within in any small temperature range ΔT is the probability density multiplied by ΔT. This type of scaling permits comparison of temperature distributors from various simulations with differing mesh sizes, geometries, etc.

Note that a remarkably small fraction of the nodes is maintained near the probe temperature, 5.0 ^{o}C above arterial temperature, owing the steep temperature gradients near the peaks. Also note the relatively tight, although skewed distribution of tissue temperatures. Although conductive heating is necessarily associated with high thermal gradients (when blood flow is high), in the present system it produces remarkably uniform tissue heating. In particular, a clear minimum temperature is established, quite near the modal (most frequent) or median temperature.

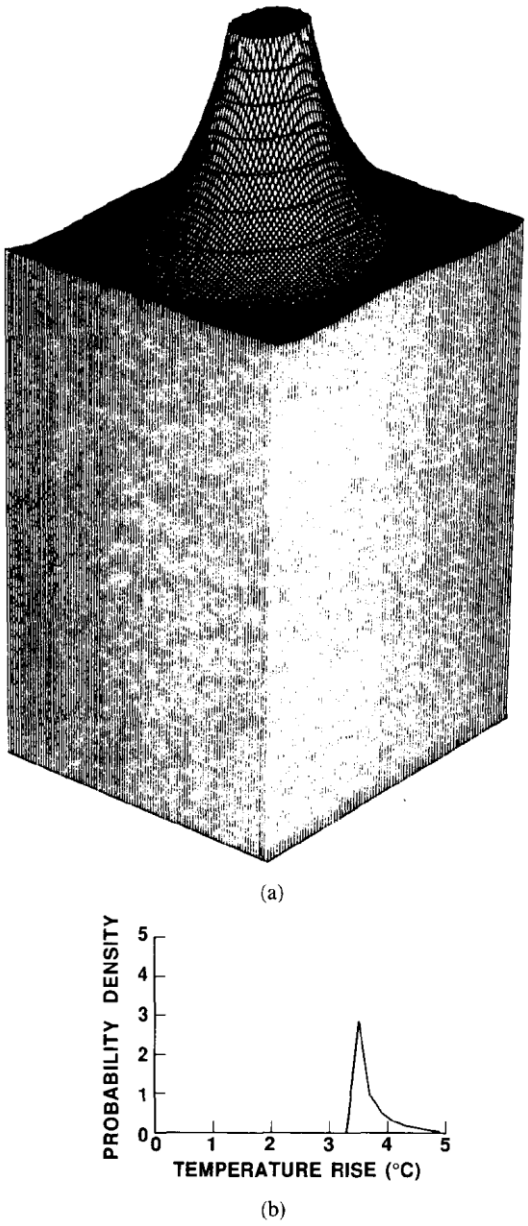

Fig. 7. High resolution, hidden line image of the tissue surrounding an interior, heated probe. Blood flow = 0.2 mL/min/g. Horizontal spacing = 1.0 cm. Vertical spacing = 0.866 cm. Probe temperature = 5.0 ^{o}C greater than arterial blood temperature. Probe diameter 0.2 cm. Tolerance = 0.001 C. Panoramic view of peak produced by combining four symmetrical quadrants. (b) Probability density function describing complete temperature distribution around one probe. Minimum temperature is close to modal (highest probability) temperature. Only a small proportion of tissue is near probe temperature.

C. Effect of Inter-catheter Spacing

The effects of heater spacing and perfusion are concisely demonstrated in histogram format. Fig. 8 illustrates histogram output for inter-catheter spacings of 1.0, 1.5, and 2.0 cm, in the presence of local blood flow equal to 0.2 mL/min/g, a value typical of tumors [35]. Note that minimal tumor temperature is lower with wider spacing, and that the distributions are somewhat less uniform. Still, most tissue is maintained near the modal temperature.

D. Effect of Perfusion

Fig. 9 shows the corresponding set of histograms for spacing uniform at 1.0 cm and blood flow ranging from 0.05 to 0.5 mL/min/g. This set of curves implies that effects of high intratumoral blood flow can be offset by raising target temperature. Because the temperature distributions are extremely skewed in the presence of high blood flow, only a small volume of tissue would be overheated by such compensatory adjustment.

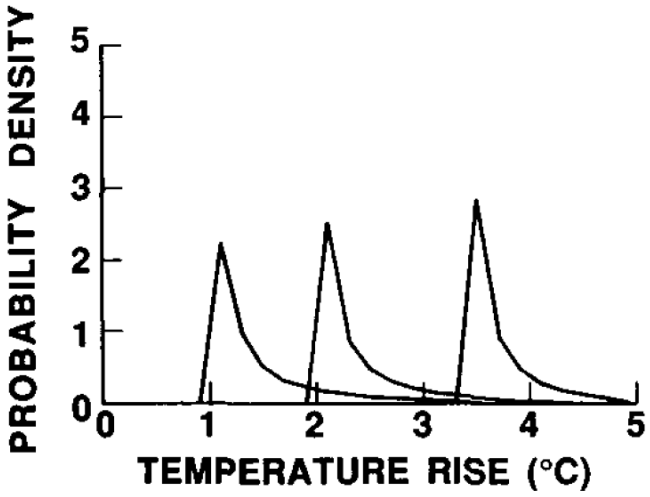

Fig. 8. Histogram output of high resolution simulation of interior probes for interprobe spacings of 1.0, 1.5, and 2.0 cm, in the presence of local blood flow equal to 0.2 mL/min/g. Other details similar to Fig. 7. Rightmost histogram represents 1.0 cm spacing. Middle histogram represents 1.5 cm spacing. Left-most histogram represents 2.0 cm spacing.

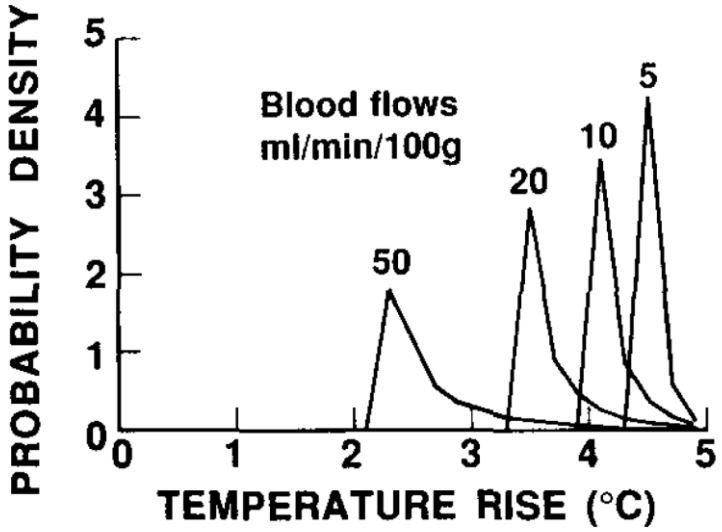

Fig. 9. Corresponding set of histograms showing the effects of blood flows ranging from 0.05 to 0.5 mL/min/g for a uniform spacing of 1.0 cm. Peaks from right to left represent perfusions of 0.05, 0.1, 0.2, and 0.5 mL/min/g, respectively. Other details similar to Fig. 7.

E. Potential for Closed-Loop Control

Fig. 10 illustrates compensation for high-blood flow by raising the target temperature of the heated probes. Target temperature was adjusted for blood flows ranging from 0.05 to 0.5 mL/min/g so that the minimum tissue temperature rise would be about 5 °C. Even though the blood flow ranged over an order of magnitude-the range expected for typical tumors-most of the tissue volume could be kept within a reasonable therapeutic range by judicious selection of the setpoint of the conductive heating elements. Most importantly, cold spots, corresponding to undertreated regions of tumor tissue can be avoided by this approach.

A simple route to closed-loop control would be obtained if it is possible to predict the central valley or minimum tissue temperature. This may be done if one knows the essential relationships between blood flow or probe spacing and minimal valley temperature relative to the probe temperature and the arterial temperature. In Fig. 11 each curve represents a given probe spacing. Minimal temperature rise for a probe setpoint 5 °C above arterial temperature is plotted as a function of perfusion. In Fig. 12 each curve represents the thermal droop, $(T_{target} - T_{min})(T_{target} - T_a)$, as a function of blood flow for a particular heater spacing. The different curves represent 1.0, 1.5, and 2.0 cm probe spacing. As perfusion increases or as probe spacing increases, the minimum tissue temperature falls toward the level of arterial temperature and the droop increases.

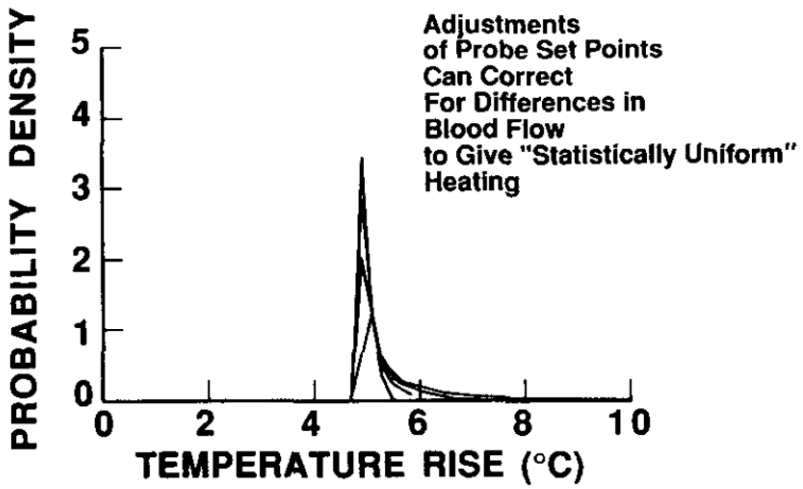

Fig. 10. Histograms for spacing uniform at 1.0 cm and blood flows ranging from 0.05 to 0.5 mL/min/g with adjustment of heated probe temperature to bring minimum tissue temperature rise to 4.7 ^{o}C. Peaks from top to bottom represent perfusions of 0.05, 0.1, 0.2, and 0.5 mL/min/g. Other details similar to Fig. 7. The algorithm for adjustment of probe temperature to obtain a desired minimum tissue temperature is presented subsequently in the text.

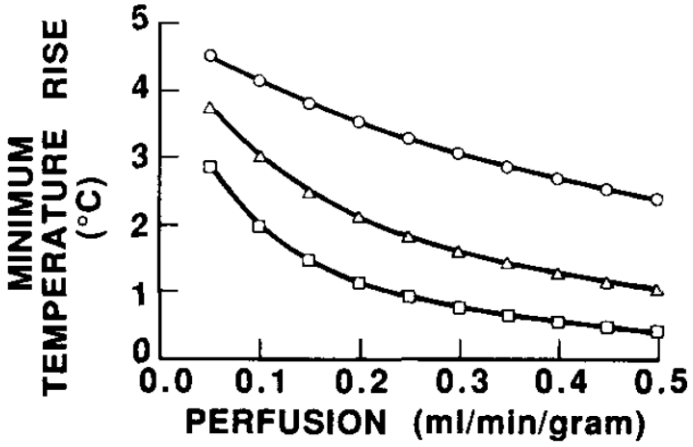

Fig. 11. Minimum temperature rise computed by the droop analysis software, plotted as a function of blood flow for various probe spacings, using a probe temperature which is 5.0 ^{o}C greater than arterial blood temperature. The different curves represent 1.0, 1.5, and 2.0 cm horizontal spacing, as defined in Fig. 8. Upper curve represents 1.0 cm spacing. Middle curve represents 1.5 cm spacing. Lower curve represents 2.0 cm spacing. The results could be proportionally scaled for probe temperature rises other than 5.0 ^{o}C.

Fortunately with the interstitial conductive heating system, perfusion in the neighborhood of each interior probe can be determined without additional invasive procedures by measuring power required to maintain each interior probe at the target temperature. Fig. 13 presents the relationships between the power required to maintain 0.1 cm radius interior probes at 5 °C above arterial temperature and the local blood flow for various probe spacings. These relationships can be known in advance from computer simulations and verified by experiment. Thus, knowing the steady-state power required to maintain an interior probe at its set point, and knowing the probe spacing, one can calculate the expected droops of the temperature distributions using the relationships in Figs. 12 and 13.

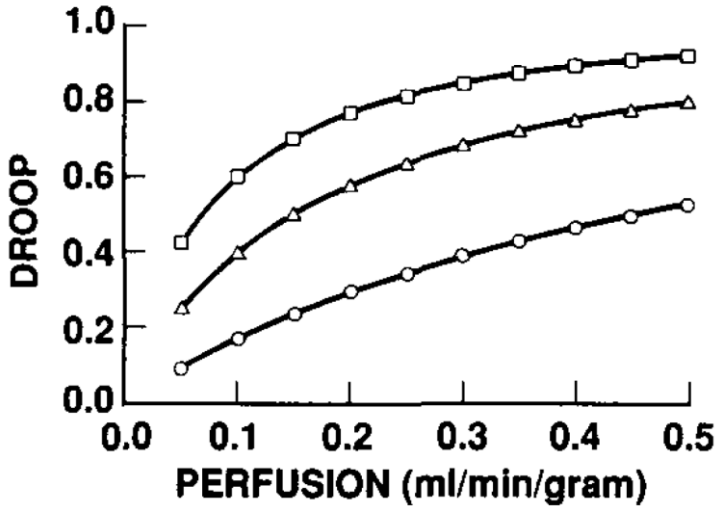

Fig. 12. Droop, defined as the minimum tissue temperature rise expressed as a fraction of maximal temperature rise, plotted as a function of blood flow for various probe spacings. The different curves represent 1.0, 1.5, and 2.0 cm horizontal spacing, as defined in Fig. 8. Upper curve represents 2.0 cm spacing. Middle curve represents 1.5 cm spacing. Lower curve represents 1.0 cm spacing.

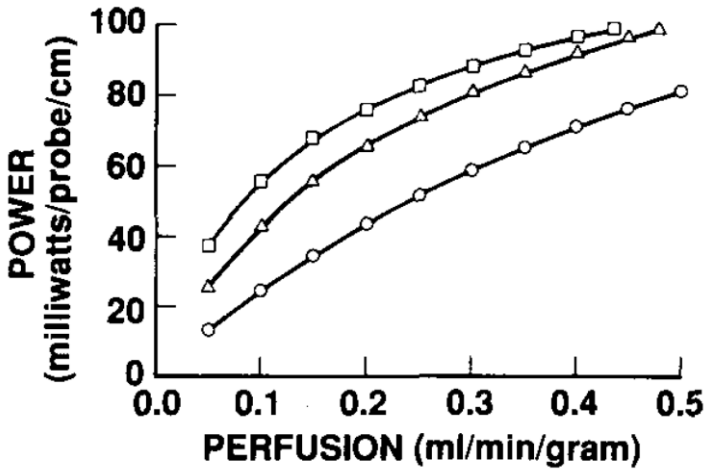

Fig. 13. Steady-state power dissipated in tissue by an interior probe, expressed as watts per cm of probe length, and plotted as a function of perfusion for 1.0, 1.5, and 2.0 cm horizontal probe spacing. Computations were done with the "droop" simulation program. Upper curve represents 2.0 cm spacing. Middle curve represents 1.5 cm spacing. Lower curve represents 1.0 cm spacing.

This ability to calculate the expected minimum temperature and droop for any particular combination of spacing and blood flow leads to a simple and effective scheme for feedback control of tissue temperature distributions. The principle is to adjust the set point of each probe to maintain the computed minimum tissue temperature in the neighborhood of the probe at a desired level. The adjustment is easily made after recognizing that the thermal droop in independent of the Target value selected. This constancy of the droop can be easily demonstrated in simulation. Rearranging defining expression for droop gives

$$\text{Target} = \frac{T_{\text{min}} - \text{droop } T_a}{1 - \text{droop}}.$$

Having estimated the droop from the steady-state probe power and the relationships in Figs. 11 and 12 for the prevailing probe spacing, one can solve for the set point necessary to produce the desired minimum tissue temperature T_{min}.

The result will be distributions like those shown in Figure 10 for the case of desired $T_{min} = 5.0$ ^{o}C. Indeed, the curves in Fig. 10 were obtained by calculated adjustment of probe temperature by the process just described. This process can be repeated to continually readjust the system for treatment induced changes in tumor blood flow.

4. DISCUSSION

Computer simulation of the temperature distributions produced by conductive heating provides insights and analyses that are very difficult to obtain experimentally, especially in a clinical setting. Chief among these is the ability to map temperatures at every point of interest in space, and thus to know the entire temperature distribution. Experimental thermometry with implanted sensors in animal or clinical studies can sample temperature at only a few discrete points. Such samplings can be especially misleading when high thermal gradients are involved, as in the present case of conductive heating.

The results of computer simulation of complete steady-state temperature distributions revealed not only the interesting properties of temperature distributions created by conductive heating of perfused tissues, but also the power and clarity of histogram analysis, and a potential method for simple feedback control of conductive heat therapy. The results reveal that the conductive heating approach is capable of generating therapeutic temperature distributions in tissue, if the spacing of heated probes is adequately close and if blood flow to the tissue is not excessively great. In a large array of probes, the outermost probes create an adiabatic boundary, which minimizes heat loss from the interior of the treated region to surrounding cooler tissues. Thus, the major route for heat loss from the bulk of the treated region is via blood flow.

Histogram analysis reveals that the temperature distributions produced by arrays of heated probes are remarkably uniform. When blood flow is low, for example 0.05 mL/min/g or less, conductive heat transfer from the probes to the interstices of the array raises tissue temperature to a level close to probe temperature. When blood flow is high, for example 0.25 mL/min/g or greater, steep thermal gradients near the probes develop, but the vast majority of tissue volume equilibrates at a relatively uniform temperature, intermediate between probe temperature and arterial blood temperature. Only a small fraction of the treated tissue remains near the probe set point temperature when blood flow is high. This later characteristic permits an extremely simple algorithm to be used for control of minimal tissue temperature to any desired level by calculated adjustment of the set points of individual probes.

Even nominally ‘‘noninvasive” external power applicators for microwave, ultrasound, or radiofrequency current require multipoint thermometry to ensure that adequate temperatures are achieved during hyperthermia. This constraint requires implantation of temperature sensors within the treated tissue since noninvasive thermometry of interstitial temperature is unavailable. If sensors are to be implanted, implantation of catheters which sense and are also capable of delivering heat may not represent a radical departure in the degree of invasiveness required for practical hyperthermia. In this sense interstitial power application may not significantly increase risk to the patient.

The present study, of course, is a theoretical one, carried out in two dimensions. In clinical practice there are likely to be variations in temperature along the lengths of the heated catheters due to differences in blood flow. Hence the uniformity of temperatures predicted in our two dimensional model is likely to be greater than that achieved in physical systems. Although temperature variation along the lengths of catheters could be overcome, at the cost of technical complexity, by independently controlling power along the length of each catheter; the

cost/benefit of such a design has yet to be explored. Similarly, in clinical implantations the spacing of catheters is not necessarily as uniform as that in the computer simulations, and, as shown in Fig. 8, such variability could significantly change expected tissue temperatures. Nevertheless, we feel that in a fundamental sense, significantly greater uniformity of tissue temperatures can be gained by the conductive interstitial approach.

The temperature distributions produced in the present simulations are similar to those produced by inductively heated ferromagnetic seeds [25], [30], [31]. However, the physical system modeled works quite differently. Electrically heated catheters contain resistive heating elements that are hard wired to a bedside control unit. The core temperature of each probe is continually monitored and can be adjusted continuously under computer control. Thus, the power applied to the probes and their temperatures can be changed, under the direction of a control algorithm to compensate for differing initial values of blood flow and also for changing blood flow in the tissue during treatment.

The constant temperature ferromagnetic seeds described by Brezovich [31] rise to the Curie point temperature, which is not continuously adjustable during a treatment session. This difference has significant implications for computer control. In particular, using an approach such as we have outlined, it is possible for a computer controlled system to continuously adjust probe temperatures in the array to achieve a desired minimum tissue temperature in the tumor, despite changes in tumor blood flow (Fig. 10). Self-regulating, constant temperature ferromagnetic seeds cannot be controlled in this way. Although ferromagnetic seeds do absorb more power as tissue perfusion increases [31], this effect is felt sufficient to maintain minimum temperatures at a desired level.

The present paper demonstrates that source temperature must be increased in the face of increased blood flow in order to maintain minimum tumor temperature. This potential or adjusting probe power to achieve more uniform minimal temperatures is a major reason for continued investigation of resistively heated interstitial probes for heat therapy of cancer.

REFERENCES

[1] G. Crile, “Selective destruction of cancers after exposure to heat,” Ann. Surg., vol. 156, no. 3, pp. 404-407, 1962.

[2] H. H. LeVeen, S. Wapnick, V. Piccone, G. Falk, and N. Ahmed, “Tumor eradication by radiofrequency therapy: Response in 21 patients,” JAMA, vol. 235, no. 20, pp. 2198-2200, 1976.

[3] F. K. Storm, W. H. Harrison, R. S. Elliott, and D. L. Morton, “Normal tissue and solid tumor effects of hyperthermia in animal models and clinical trials,” Cancer Res., vol. 39, no. 6, pp. 2245-2250, 1979.

[4] H. H. LeVeen, N. Ahmed, V. A. Piccone, S. Shugaar, andG. Falk, “Radio-frequency therapy: Clinical Experience,” Ann. NY Acad. Sci., vol. 335, pp. 362-371, 1980.

[5] N. B. Hornback, R. Shupe, H. Shidnia, B. T. Joe, E. Sayoc, R. George, and C. Marshall, "Radiation and microwave therapy in the treatment of advanced cancer," Radiol., vol. 130, pp. 459-464, 1979.

[6] E. W. Hahn and J. H. Kim, "Clinical observations on the selective heating of cutaneous tumors with the radio-frequency inductive method," Ann. NY Acad. Sci., vol. 335, pp. 347-351, 1980.

[7] U. Raymond, K. T. Noell, K. T. Woodward, B. T. Worde, R. I. Fishburn, and L. S. Miller, "Microwave-induced local hyperthermia in combination with radiotherapy of human malignant tumors," Cancer, vol. 45, pp. 638-646, 1980.

[8] J. L. Meyer, "Hyperthermia as an anticancer modality-A historical perspective," Front Radiat. Ther. Onc., vol. 18, pp. 1-22, 1984.

[9] B. Mondovi, R. Strom, G. Rotilio, A. Agro, R. A. Cavaliere, and A. Rossi-Fanelli, "The biochemical mechanism of selective heat sensitivity of cancer cells I: Studies on cellular respiration," Europ. J. Cancer, vol. 5, pp. 129-136, 1969.

[10] R. Cavaliere, E. C. Ciocatto, B. C. Giovanella, C. Heidelberger, R. O. Johnson, M. Margottini, B. Mondovi, G. Moricca, and A. Rossi-Fanelli, "Selective heat sensitivity of cancer cells-Biochemical and clinical studies," Cancer, vol. 20, no. 9, pp. 1351-1381, 1967.

[l l] B. C. Giovanella, A. C. Morgan, J. S. Stehlin, and L. J. Williams, "Selective lethal effect of supranormal temperatures on mouse sarcoma cells," Cancer Res., vol. 33, pp. 2568-2578, 1973.

[12] C. W. Song, M. S. Kang, J. G. Rhee, and S. H. Levitt, "The effect of hyperthermia on vascular functions, pH, and cell survival," Radiol., vol. 137, pp. 795-803, 1980.

[13] M. S. Kang, C. W. Song, and S. H. Levitt, "Role of vascular function in response of tumors in vivo to hyperthermia," Cancer Res., vol. 40, pp. 1130-1135, 1980.

[14] L. Gerweck and E. Rottinger, "Enhancement of mammalian cell sensitivity to hyperthermia by pH alteration," Radiat. Res., vol. 67, pp. 508-511, 1976.

[15] W. C. Dewey and M. L. Freeman, "Rationale for use of hyperthermia in cancer therapy," Ann. NY Acad. Sci., vol. 335, pp. 372-378, 1980.

[16] M. W. Dewhirst, D. A. Sim, S. Sapareto, and W. G. Connor, "Importance of minimum tumor temperature in determining early and long term responses of spontaneous canine and feline tumors to heat and radiation," Cancer Res., vol. 44, pp. 43-50, 1984.

[17] C. F. Babbs, J. R. Oleson, and J. A. Pearce, "Equipment for local hyperthermia therapy of cancer," Med. Instrument., vol. 16, pp. 245- 248, 1982.

[18] P. F. Turner, "Regional heating with an annular phased array," IEEE Trans. Biomed. Eng., vol. BME-31, pp. 106-114, 1984.

[19] F. A. Gibbs, "Clinical evaluation of a microwave/radiofrequency system (BSD corporation) for induction of local and regional hyperthermia," J. Microwave Power, vol. 16, pp. 185-192, 1981.

[20] J. J. W. Lagendijk, "A new coaxial TEM radiofrequency microwave applicator for noninvasive deep-body hyperthermia,'' J. Microwave Power, vol. 18, pp. 367-376, 1983.

[21] P. P. Lele and K. J. Parker, "Temperature distributions in tissues during local hyperthermia by stationary or steered beams of unfocussed or focused ultrasound," Brit. J. Cancer (Suppl. V), vol. 45, pp. 108-121, 1982.

[22] B. C. Burckhardt, P. A. Grandchamp, and H. Hoffman, "Focusing native method," IEEE Trans. Sonics Ultrason., vol. SU-22, pp. 11- 15, 1975.

[23] K. Hynynen, D. J. Watmough, and J. R. Mallard, "Design of ultrasonic transducers for local hyperthermia," Ultrasound Med. Biol., vol. 7, pp. 397-402, 1981.

[24] J. M. Vaeth, Ed., Frontiers of Radiation Therapy and Oncology Vol. 18-Hyperthermia and Radiation Therapy/Chemotherapy in the Treatment of Cancer. Karger, Basel, 1983.

[25] J. W. Strohbehn and J. A. Mechling, "Interstitial techniques for clinical hyperthermia, Chapter 5," in Physical Techniques in Clinical Hyperthermia, J . W. Hand and J. R. James, Eds. New York: Wiley, 1986. pp. 210-287.

[26] A. J. Milligan and R. R. Dobelbower, "Interstitial hyperthermia," Med. Instrument., vol. 18, pp. 175-180, 1984.

[27] M. B. Lilly, I. A. Brezovich, and W. J. Atkinson, "Hyperthermia induction with thermally self-regulating ferromagnetic implants," Radiol., vol. 154, pp. 243-244, 1985.

[28] C. T. Coughlin, T. Z. Wong, J. W. Strohbehn, T. A. Colacchio, J. E. Sutton, R. Z. Belch, and E. B. Douple, "Intraoperative interstitial microwave induced hyperthermia and brachytherapy, " Int. J . Rad. Oncol. Biol. Phys., vol. 11, pp. 1673-1678, 1985.

[29] I. A. Brezovich, W. 3. Atkinson, and M. B. Lilly, "Local hyperthermia with interstitial techniques," Cancer Res. (Suppl.) vol. 44, pp. 4752-4756, 1984.

[30] A. Y. Matloubieh, R. B. Roemer, and T. C. Cetas, "Numerical simulation of magnetic induction heating of tumors with ferromagnetic seed implants," IEEE Trans. Biomed. Eng., vol. BME-31, pp. 227- 234, 1984.

[31] I. A. Brezovich, W. J. Atkinson, and M. B. Lilly, “Temperature distributions in tumor models by self-regulating nickel-copper alloy thermoseeds.” Med. Physics, vol. 11, pp. 145-152, 1984.

[32] K. E. Torrance, “Numerical methods in heat transfer,” in Handbook of Heat Transfer Fundamentals, W. M. Rohsenow, Ed. New York: McCraw-Hill, 1985, pp. 5.1--5.18.

[33] F. P. Incropera and D. P. Dewitt, Fundamentals of Heat Transfer. New York: Wiley, 1981.

[34] M. M. Chen and K. R. Holmes, “Microvascular contributions in tissue heat transfer,” Ann. NYAcad. Sci., vol. 335, pp. 137-150, 1980.

[35] H.I. Peterson, Tumor Blood Flow Compared with Normal Tissue Blood Flow. Boca Raton. FL: CRC Press. 1979. DD. 103-114.